



A Comprehensive Corrosion Inhibition Behaviour Studies of *Leucophyllum frutescens* Leaves Extract for Mild Steel

S. MANIMEGALAI^{1,*}, A. PRITHIBA², G. KANTHIMATHI³ and A. MATHINA²

¹Department of Chemistry, Arulmigu Palaniandavar College of Arts and Culture, Palani-624601, India

²Department of Chemistry, Avinashilingam Institute for Home Science and Higher Education for Women, Coimbatore-641043, India

³Department of Chemistry, Ramco Institute of Technology, Rajapalayam-626117, India

*Corresponding author: E-mail: mani_megalai22@yahoo.in

Received: 8 June 2024;

Accepted: 16 July 2024;

Published online: 30 August 2024;

AJC-21732

In an effort to address corrosion in an environmentally conscious manner, a current study has investigated the efficacy of an acid extract derived from *Leucophyllum frutescens* leaves as a green corrosion inhibitor for mild steel in acidic conditions (1.0 M HCl solution). The investigation, conducted at room temperature using standard mass loss and electrochemical techniques, varied the extract concentration, temperature and immersion time. Through these experiments, an adsorption isotherm was established and kinetic and thermodynamic parameters were evaluated. The electrochemical measurements suggested a mixed mode of inhibition. Surface analytical techniques including FT-IR, UV-visible, SEM and 3D optical profilometer were employed to confirm the inhibitor's effectiveness in preventing corrosion by protecting the mild steel surface and impeding hydrogen evolution and metal dissolution. The findings indicate that *L. frutescens* leaves extract offers promising corrosion protection while being environmental friendly due to its biodegradability and lack of harmful substances such as heavy metals.

Keywords: *Leucophyllum frutescens*, Electrochemical studies, Thermodynamic parameters, Corrosion inhibition.

INTRODUCTION

Throughout history, corrosion, the breakdown of materials due to chemical reactions with their surroundings, has persistently posed significant challenges. In contemporary times, heightened focus on metallic corrosion is imperative due to its potential ramifications: costly repairs for machinery and infrastructure, product contamination expenses, environmental degradation and potentially jeopardized human safety [1,2]. The focus of researchers [3-6] has been on using inhibitors to prevent metals from corroding. In industrial sector, the corrosion inhibitors are commonly employed to manage dissolution and lower the rate of corrosion when exposed to strong acid solutions. Organic compounds with oxygen, sulphur and nitrogen in their molecules make up the majority of acid inhibitors [7,8]. One of the qualities of a corrosion inhibitor is its ability to reduce corrosion rates. Its active principle must come into touch with the metal in order to protect it and avoid negative side effects [9,10]. Their biodegradability, eco-friendliness, affordability, lack of toxicity

and ease of availability have made their use a more popular trend in recent years. More study has been done to develop green inhibitors that are acceptable to the environment [11-15].

The evergreen shrub *Leucophyllum frutescens* belongs to the Scrophulariaceae family of figworts and is endemic to the states of Coahuila, Nuevo León and Tamaulipas in Northern Mexico as well as the Texas state of United States. The antinociceptive properties and phytochemical composition of a crude ethanolic extract obtained from *Leucophyllum frutescens* roots were investigated [16]. Phytochemical analysis identified the presence of steroids, tannins and alkaloids in the ethanolic extract [17]. Further fractionation of the methanolic root bark extract led to the isolation of compounds such as leubethanol, biflorin, etc., indicating a serrulatane-type diterpene with activity against both drug-sensitive and drug-resistant strains [18].

Due to the presence of long alkyl chain (*n*-heneicosane) and droepingaione, an oxygenated sesquiterpene majorly [19], therefore, in this study, the anticorrosion properties of aqueous leaves extract of *Leucophyllum frutescens* plant is investigated

for mild steel in acidic conditions (1.0 M HCl). Various parameters like effect of temperature using weight loss, Tafel polarization, linear polarization resistance (LPR), electrochemical impedance (EIS) were determined.

EXPERIMENTAL

Leaves of *Leucophyllum frutescens* plant were collected from the local nursery of Coimbatore, India. The plant was authenticated by the Herbarium, Avinashilingam Institute for Home Science and Higher Education for Women, Coimbatore, India. The mild steel containing the compositions of C 0.089%; Mo 0.021%; S 0.019%; Fe 99.58%; Mn 0.215% and P 0.017% was utilized for the present research work. Chemicals, such as hydrochloric acid and acetone of reagent grade were purchased from Sigma-Aldrich, USA. Distilled water was obtained using a Millipore Milli-Q system and used throughout the experiments. Biologic EC Lab version 10.23 facilitated the electrochemical measurements.

Characterization: The FT-IR spectra of *Leucophyllum frutescens* leaves (LFL) powder were recorded in the range of 4000–400 cm^{-1} using a Perkin-Elmer FT-IR spectrophotometer fitted with the SOFTWARE - OPUS version 6.5. The UV absorption studies were conducted before the submersion of metal in 1 M HCl for 3 h, both with and without the addition of 0.7% LFL inhibitor using a Jasco-V630 spectrophotometer in the range from 800 to 200 nm. The JEOL MODEL JSM 6360 SEM was utilized to analyze the morphology of the metal surface. A Zeta-20 3D Optical Profiler was used to examine surface profiles and pores of the mild steel specimens.

Preparation of mild steel sample: Mild steel (MS) needs to be safe guarded because it corrodes badly in a hostile environment. Using a big mild steel sheet, regular samples measuring 1 cm \times 5 cm were used. The specimen was drilled in order to prepare it for weight loss analysis. After that it underwent mechanical polishing, degreasing, cleaning with de-ionized water and thorough drying.

Preparation of inhibitor: A 25 g of dried leaves were refluxed for 3 h in 500 mL of HCl to obtain *Leucophyllum frutescens* leaves (LFL) extract, which was then refrigerated overnight. The cooled extract was filtered and 500 mL of 1 M HCl were added to make an extract with a 5% inhibitor.

Phytochemical screening: Standard procedures were used when performing phytochemical analysis on the extract [20].

Mass loss techniques: Pre-weighed coupons were submerged in triplicate, with and without an inhibitor, in a beaker containing 100 mL of 1 M HCl acid for a predefined amount of time. A glass hook supported the coupons, then washed, dried and reweighed the coupons. It was observed the average mass loss of coupons. A range of parameters were tested, including temperature (303–353 K), the concentration ranges from 0.1% to 0.7% and the immersion times were 30, 60, 180, 360, 720 and 1440 min.

Determination of corrosion rate (CR): The widely used expression is measured in milli inches per year using formula:

$$\text{C.R (mpy)} = \frac{3.45 \times 10^6 \times W}{D \times A \times T} \quad (1)$$

where A is the sample area in cm^2 , T is the exposure duration in h, W is the weight loss in g; and D is the mild steel density in g/cm^3 .

Surface coverage and inhibition percentage calculations: The surface coverage (θ) and inhibitory efficiency (IE) percentage were calculated using the following formula:

$$\text{IE (\%)} = \frac{W_0 - W}{W_0} \times 100 \quad (2)$$

$$\theta = \frac{W_0 - W}{W_0} \times 100 \quad (3)$$

whereas the corrosion rate in g is represented by W_0 the rate without inhibitor and W, the rate with inhibitor.

Thermodynamic parameters determination: Eqn. 4 can be used to find the change in free energy (ΔG) of the inhibitors' adsorption [21].

$$\log C = \left(\frac{\log \theta}{(1 - \theta)} \right) - \log B \quad (4)$$

In this case, $\log B = -1.74 - (\Delta G/2.303 RT)$, T is the temperature in Kelvin; R is the gas constant (8.314 J/mol) and C is the inhibitor concentration. The values of the enthalpy of adsorption (ΔH) and entropy of adsorption (ΔS) were obtained using the Gibb's Helmholtz equation.

$$\Delta G = \Delta H - T\Delta S \quad (5)$$

Adsorption isotherms: The adsorption isotherms have been used to study inhibitor-metal surface interaction. Two types of isotherms viz. (i) Langmuir [$\log (\theta/(1-\theta))$ vs. $\log C$]; and (ii) Temkin (θ vs. $\log C$) were employed to establish the isotherms most appropriate to the experimental data [22].

Activation energy (E_a): An Arrhenius plot calculated activation energy at varied inhibitor dosages by plotting temperature and $\log CR$ vs. $1/T$. Eqn. 6 was used to calculate activation energy (E_a) based on the slope.

$$E_a = -2.303 \times R \times \text{slope of Arrhenius plot} \quad (6)$$

In order to obtain more details on the corrosion process (CR), activation kinetic parameters such activation energy (E_a); enthalpy (ΔH) and entropy (ΔS) were also evaluated from the effect of temperature using Arrhenius law (eqn. 7):

$$\text{CR} = \frac{RT}{Nh} \exp\left(\frac{\Delta S_a}{R}\right) \exp\left(\frac{\Delta H_a}{R}\right) \quad (7)$$

where h is the Planck's constant; N is the Avogadro number; ΔS_a is the activation entropy and ΔH_a is the activation enthalpy.

Electrochemical measurements: The electrochemical experiments were conducted using standard three-electrode cells. The working electrode consisted of the sample, while a saturated calomel electrode (SCE) and a platinum foil counter electrode served as the reference and counter electrodes, respectively. Prior to initiating measurements, a settling period of 30 min was allowed for the electrode potential. Polarization experiments, scanning the corrosion potential at a rate of 2 mV/s between -0.1 and -1 mV, were conducted both with and without the inhibitor. The electrochemical tests were carried out on a polished mild steel surface with dimensions measuring 1 cm^2 .

Tafel plot: For Tafel plot, the corrosion potentials in both the cathodic and anodic electrodes across a range of several hundred millivolts are measured. It is expected that the intersection of the log current linear region and applied potential will occur. The Tafel slopes (b_a and b_c), indicative of the linear region's slope, also define the corrosion potential (E_{corr}) and current (I_{corr}). The inhibitory efficiency (IE) was calculated using the eqn. 8:

$$IE (\%) = \frac{I_{\text{corr}}(\text{blank}) - I_{\text{corr}}(\text{inhibited})}{I_{\text{corr}}(\text{blank})} \times 100 \quad (8)$$

Using the linear polarization resistance (LPR) method, the inhibitory efficiency (IE %) can be calculated as follows:

$$IE (\%) = \frac{R_p(\text{inhibited}) - R_p(\text{blank})}{R_p(\text{inhibited})} \times 100 \quad (9)$$

where R_p (inhibited) and R_p (blank) stand for linear polarization resistance in the presence and absence of inhibitor, respectively.

EIS analysis: The electrochemical impedance spectroscopic (EIS) studies were conducted by applying AC signal with a amplitude of 5-10 mV and a frequency range of 10 KHz to 10 MHz. The formula can be used to determine the I.E.

$$IE (\%) = \frac{R_{\text{ct}}(\text{inhibited}) - R_{\text{ct}}(\text{blank})}{R_{\text{ct}}(\text{inhibited})} \times 100 \quad (10)$$

where, R_{ct} (blank) and R_{ct} (inhibited) stand for charge transfer resistance in the presence and absence of the inhibitor, respectively. To compute surface coverage (θ), eq. 11 was used.

$$\theta = 1 - \frac{C_{\text{dl}}(\text{inhibited})}{C_{\text{dl}}(\text{blank})} \quad (11)$$

where C_{dl} (blank) and C_{dl} (inhibited) stand for the double layer capacitance in the inhibitor-free and inhibitor-filled conditions, respectively.

RESULTS AND DISCUSSION

Mass loss measurements: Experiments were carried out by varying acidic extract concentration of LFL (0.1% to 0.7% extract) in order to investigate the impact of inhibitor on the mild steel submerged in 1 M HCl medium. Fig. 1 showed that the concentration of inhibitor affected the rate of corrosion. The reason is due to their adsorption onto the surface of metal, thus, the LFL extract are found to be effective to inhibit the

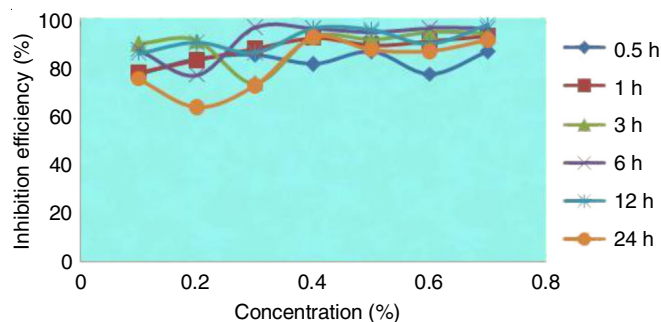


Fig. 1. A plot of concentration vs. IE in 1 M HCl

mild steel corrosion. As concentration increased, the adsorption process effectively hindered the dissolution of metal corrosion sites, hence decrease the mass loss. At different immersion intervals of time, the efficacy of inhibition increased as the inhibitor's level increased. According to the results (Table-1), the corrosion of mild steel may be inhibited by the inhibitor molecules covering its surface for a longer time period during immersion. A high of 98.2% inhibition was reached at 0.7% of extract after 12 h of immersion. Therefore, it was observed that the LFL extract behaved consistently throughout all immersion periods.

Effect of temperature: Depending on the temperature, mild steel and acid might interact differently both in presence and absence of inhibitor. Mass loss studies were performed at different temperatures ranging from 303 to 353 K. It was evident that the rate of corrosion increases as temperature rose in both the corrosive media. However, when compared to blank, it was found that the presence of the inhibitor effectively suppressed the corrosion rate (Fig. 2), which further confirmed that the corrosion inhibition could be due to the adsorption (Table-2).

Adsorption isotherms: Organic compounds adsorb through donor-acceptor interactions between relatively loosely bound electrons, such as from anions and organic molecules and/or heterocyclic compounds with lone pair electrons or π -electrons and the vacant d -orbitals of metallic atoms. The adsorption process or inhibitory activity may be affected by specific factors, such as size of the organic molecule, number of functional groups and the polarity that facilitates the formation of a strong bond or the rate at which inhibitor compounds adhere to the surface. The Langmuir adsorption isotherm provides a fundamental mechanism of the adsorption procedure and can be represented as follows:

TABLE-1
EFFECT OF ACIDIC EXTRACT OF LFL CONCENTRATION AND IMMERSION PERIOD IN 1 M HCl ON MILD STEEL

Conc. (%)	Rate of corrosion and effectiveness of inhibition											
	0.5 h		1 h		3 h		6 h		12 h		24 h	
	CR (mpy)	IE (%)	CR (mpy)	IE (%)	CR (mpy)	IE (%)	CR (mpy)	IE (%)	CR (mpy)	IE (%)	CR (mpy)	IE (%)
0.1	255	58.9	162	85.4	160	83.8	114	85.7	51	95.6	73	23.6
0.2	238	61.6	179	100.2	164	84.2	59	92.9	28	97.6	28	70.6
0.3	187	69.8	123	38.1	160	84.2	34	95.6	36	96.8	19	79.7
0.4	179	71.2	132	47.6	129	87.3	25	96.8	35	97.0	31	67.3
0.5	153	75.3	115	28.5	172	83.1	34	95.6	24	97.9	30	68.6
0.6	255	58.9	140	57.2	130	87.2	37	95.3	26	97.7	25	73.2
0.7	213	65.7	68	23.7	115	88.7	41	94.7	21	98.2	36	61.7

TABLE-2
EFFECT OF TEMPERATURE ON MILD STEEL CORROSION IMMERSED
IN 1 M HCl AT VARIOUS LFL EXTRACT CONCENTRATIONS

Conc. (%)	Corrosion rate and inhibition efficiency											
	303 K		313 K		323 K		333 K		343 K		353 K	
	CR (mpy)	IE (%)	CR (mpy)	IE (%)	CR (mpy)	IE (%)	CR (mpy)	IE (%)	CR (mpy)	IE (%)	CR (mpy)	IE (%)
Blank	622	–	2669	–	5603	–	1114	–	1008	–	2013	–
0.1	255	58.9	324	87.8	895	84.1	2140	80.7	2592	72.2	5817	71.1
0.2	238	61.6	554	79.2	1049	81.3	1253	88.7	2001	80.1	5893	70.7
0.3	187	69.8	349	86.9	571	89.8	1287	88.4	1339	86.7	3650	81.8
0.4	255	71.2	725	72.8	1143	79.7	1151	896	1748	82.6	3113	84.5
0.5	213	75.3	341	87.2	511	90.8	1142	89.7	1401	86.1	2550	87.3
0.6	179	58.9	503	81.1	622	88.8	1015	90.8	1313	86.9	2848	85.8
0.7	153	65.7	784	70.6	494	91.2	1160	89.5	1108	89.0	2806	86.1

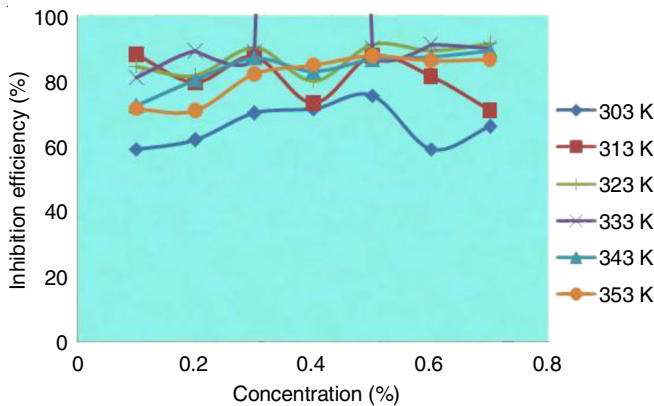


Fig. 2. Variation of IE as function of temperature (LFL) extract in 1 M HCl

$$KC = \frac{\theta}{1-\theta} \tag{12}$$

where K denotes the equilibrium constant and can be rearranged, which becomes as follows:

$$\frac{C}{\theta} = C + 1K \tag{13}$$

where C is the inhibitor concentration and K is the adsorptive equilibrium constant.

The straight lines were obtained by plotting C/θ versus C with uniform slope, which suggests that the LFL extract's adsorption on the mild steel surface followed the Langmuir adsorption isotherm. A straight line was generated when the inhibitor's surface coverage was plotted against $\log C$ vs. θ (Fig. 3). Fig. 4 shows the inhibitor's adsorption at the Temkin adsorption isotherm and mild steel acidic solution boundary.

Energy of activation (E_a): The Arrhenius equation and mass loss data were used to calculate the apparent activation energy for mild steel corrosion in 1 M HCl with and without LFL.

$$CR = Ae^{\left(\frac{-E_a}{RT}\right)} \tag{15}$$

Fig. 5 shows the linear form of the relationship between $\log CR$ and $1/T$, from which the activation energy (E_a) at different temperatures was calculated. The E_a values (Table-3) for mild steel in LFL extract in 1 M HCl medium indicated that the inhibitors were physically adsorbed onto the mild steel surface

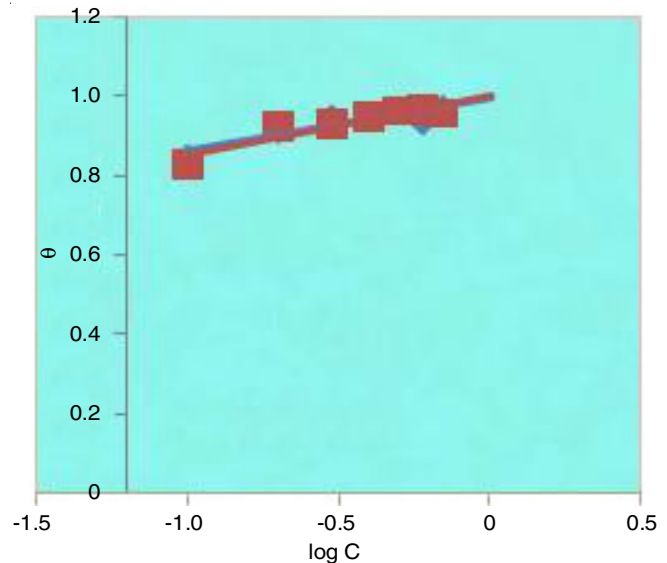


Fig. 3. Langmuir adsorption isotherm for MS/HCl/LFL

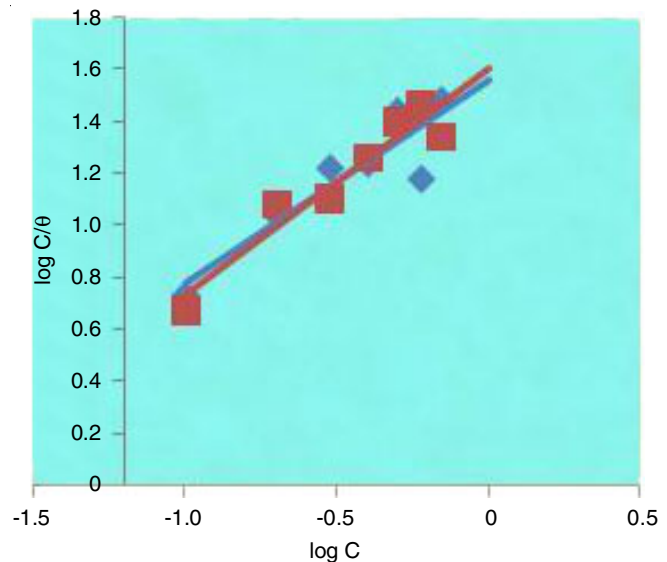


Fig. 4. Temkin adsorption isotherm for MS/HCl/LFL

supported by the weak van der Waals or electrostatic forces of attraction [23]. Moreover, the E_a values were significantly higher in inhibited systems compared to uninhibited ones.

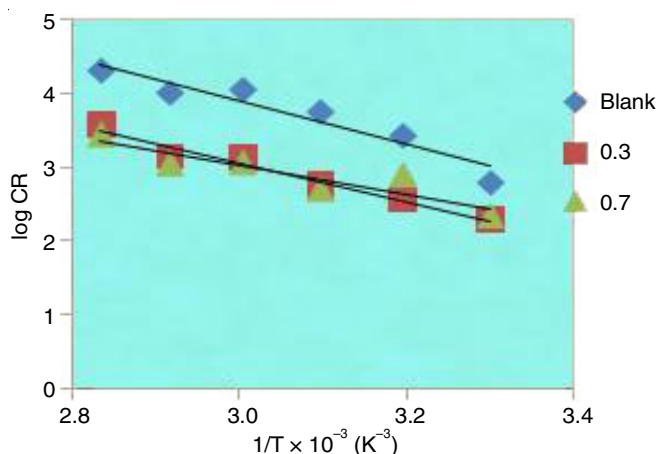


Fig. 5. Arrhenius plot for 1 M HCl with LFL/MS

TABLE-3
THERMODYNAMIC PARAMETERS OF MILD STEEL IMMERSSED IN 1 M HCl AT VARYING CONCENTRATIONS OF LFL EXTRACT

Conc. v/v (%)	$-E_a$ (KJ/mol)	ΔH_a (kJ/mol)	ΔS_a (J/mol)
Blank	59.5	59.5	46.2
0.1	60.5	60.5	36.6
0.2	53.6	53.6	15.5
0.3	52.6	52.6	9.6
0.4	46.2	46.2	-8.3
0.5	51.4	51.4	4.5
0.6	41.9	41.9	-22.9
0.7	40.3	40.3	-27.9

Activation of entropy and enthalpy: According to the transition state theory, the values of E_a and ΔH_a fluctuated similarly when different inhibitor concentrations were introduced. The positive readings of ΔH_a suggest the endothermic process, thereby confirming the inhibitor's chemical adsorption on the mild steel. The activated complex of the rate-determining phase displayed an association as opposed to the dissociation step, as demonstrated by the negative value of ΔS_a for LFL in HCl, because the reactants were replaced by the activated complex, resulted in the reduction of randomness or entropy [24].

Thermodynamic parameters: Based on eqn. 4, the ΔG values were negative both in the presence and absence of inhibitors (Table-4). This observation suggested that the adsorption behaviour of the inhibitor was spontaneous under the experimental conditions. The negative ΔG values further indicate a strong interaction between the inhibitor molecules and the metal surface. According to the general rule, ΔG values of -20 kJ/

mol or less suggest electrostatic interactions (physisorption) between charged molecules and the metal surface, while values of -40 kJ/mol or greater indicate the sharing or transfer of charge to form a coordinate bond [25] (chemisorption) with organic molecules. The studies calculated ΔG_{ads} values varied from -12 to -23 kJ mol $^{-1}$. Because of the complexity of the corrosion inhibiting process [26], there is possibility that chemical adsorption was also involved in the inhibitor molecules' adsorption, even though it is presumed that physical adsorption occurred.

Electrochemical measurements: In Fig. 6, the anodic and cathodic polarization curves of mild steel (MS) electrode in 1 M HCl medium are depicted, both with and without varying concentrations of LFL extract at 303 K. Whereas Table-5 tabulated the electrochemical parameters such as corrosion potential (E_{corr}) and corrosion current density (I_{corr}), which were determined using the anodic and cathodic Tafel slopes from the polarization curves. In the presence of LFL extract, both anodic and cathodic curves shift towards the lower current densities, thereby slowing down the corrosion rate. Furthermore, it was observed that I_{corr} values increased as the concentration of inhibition decreased. Furthermore, the values of inhibition efficiency (IE%) increased with higher concentrations of inhibitor. The LFL extract in 1 M HCl demonstrated a maximum inhibition efficiency of 83.7% at a concentration of 0.7%.

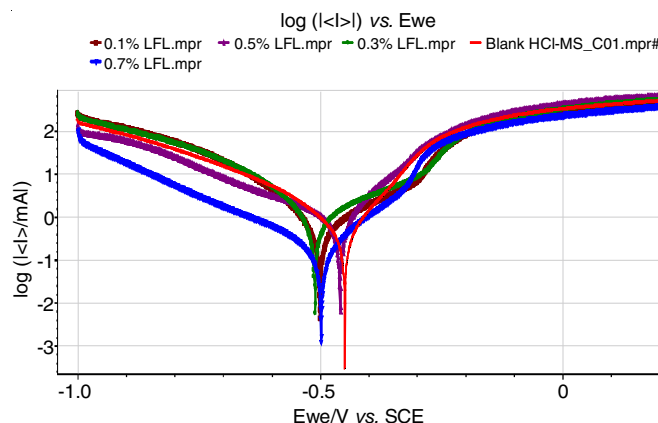


Fig. 6. Mild steel potentiodynamic polarization plots in 1 M HCl with and without LFL extract

The heterogeneous nature of the inhibitor was demonstrated by the absence of any apparent change in the E_{corr} values in presence of inhibitors. It was found that increasing the inhibitor concentrations caused the E_{corr} values to shift in favour of higher positive values, which indicated that coating on the

TABLE-4
THERMODYNAMIC PARAMETERS OF MILD STEEL IMMERSSED IN 1 M HCl AT VARIOUS LFL EXTRACT CONCENTRATIONS

Inhibitor's conc. v/v (%)	Adsorption free energy: ΔG (kJ/mol)						ΔS (J/mol)	ΔH (kJ/mol)
	303 K	313 K	323 K	333 K	343 K	353 K		
0.1	16.8	21.5	21.4	21.4	21.0	20.5	-49.1	-4.3
0.2	15.3	18.1	19.0	21.3	19.9	18.5	-68.2	3.6
0.3	15.2	18.5	19.8	20.1	20.2	19.2	-71.4	4.5
0.4	14.6	15.4	16.9	19.6	18.4	18.8	-94.4	13.6
0.5	14.6	17.2	18.7	19.1	18.6	18.9	-73.2	6.1
0.6	12.2	15.5	17.7	18.8	18.3	18.1	-108.7	18.8
0.7	12.6	13.6	17.9	18.1	18.4	17.6	-112.5	20.5

TABLE-5
ELECTROCHEMICAL POLARIZATION PARAMETERS OF MILD STEEL
IMMERSED IN 1 M HCl AT VARYING CONCENTRATIONS OF LFL EXTRACT

Conc. of inhibitor (%)	Polarization parameters					Linear polarization resistance parameters	
	E_{corr} (mV/SCE)	I_{corr} (A/cm ²)	b_a (mV/decade)	b_c (mV/decade)	IE (%)	R_p (Ohm/cm ²)	IE (%)
Blank	-457	584	85.3	172		3.4	
0.3	-476	210	80.4	134	64.1	46.8	92.1
0.1	-467	340	112	144	41.7	24.4	86.1
0.5	-435	140	77.4	151	76.2	47.2	92.7
0.7	-478	95	98	165	83.7	175	98.1

metal surface slowed its breakdown. In general, an inhibitor is categorized as either cathodic or anodic type if its presence causes a change in corrosion potential (E_{corr}) of greater than 85 mV relative to its absence. But in this case, the E_{corr} values changes were less than 85 mV, indicated that they prevent mild steel corrosion in 1 M HCl acid solution [27] because of the heterogeneous nature of the inhibitor. In acidic solutions, it was indicated that R_p values increased as the inhibitor's concentration increased and the highest efficiency for extract in 1 M HCl was found to be 98.1%. The inhibitory activity was hypothesized to be caused by the adsorption and formation of a barrier layer on the metal surface, which separates the metal surface from the corrosive medium.

Electrochemical impedance spectroscopy (EIS) studies:

Fig. 7 illustrates the impedance responses of mild steel in 1 M HCl system in Nyquist (a), Bode modulus (b) and phase angle (c) formats, with varying concentrations of LFL extract. The Nyquist plots for both HCl medium, with and without LFL, exhibited similar the morphologies indicating that the addition of the extract did not alter the corrosion process's mechanism. The presence of a single capacitive semicircle with centers below the real axis [28] in the Nyquist plots suggests that the corrosion process is primarily governed by charge transfer mechanisms.

In the Bode charts, the semicircle diameter increased with the inhibitor concentration, possibly due to the mild steel surface's higher inhibitory molecule coverage. A solid electrode with depressed semicircles shows frequency dispersion, which is commonly caused by contaminants, grain boundaries, surface roughness, homogeneity and surface-active site distribution. The decrease in C_{dl} values indicates that LFL act *via* adsorption at the mild steel interface, which may be attributed to a decrease

in the local dielectric constant or an increase in the electrical double layer's thickness (Table-6). According to phase-angle and Bode modulus data, LFL concentration increases absolute impedance at low frequencies, indicating that LFL components adhere to the mild steel surface and increase protection.

TABLE-6
IMPEDANCE PROPERTIES OF MILD STEEL
CORROSION IMMERSSED IN 1 M HCl AT
VARIOUS LFL EXTRACT CONCENTRATIONS

Conc. (%)	R_s (Ω cm ²)	R_{ct} (Ω cm ²)	IE (%)	C_{dl} ($\mu\text{F}/\text{cm}^2$)	θ
Blank	1.4	12.6	–	773	–
0.1	2.9	115	89.0	219	0.72
0.3	3.2	128	90.2	148.7	0.81
0.5	3.1	154	91.8	119	0.85
0.7	4.1	162	92.2	53.9	0.93

Surface analysis

FT-IR studies: Fig. 8 shows the FTIR spectrum of the protective layer adsorbed on mild steel after submerging it in 1 M HCl with LFL extract. In the FTIR spectrum of *L. frutescens* leaves (LFL) extract (Fig. 8), the O-H stretching is responsible for the unusually strong wide band observed at 3516 cm⁻¹. The strong band at 1643 cm⁻¹ is associated with the C=O stretching vibration, whereas the absorption band at 2924 cm⁻¹ is linked to the –CH asymmetrical stretching vibration [22]. Thus, phytochemicals with several oxygen and nitrogen atoms in aromatic rings and functional groups (*e.g.* polyphenols, flavonoids, steroids, *etc.*) provides the active sites for the adsorption of LFL extract as inhibitor on the surface of mild steel surface. As compared to FTIR spectrum of LFL extract, a broad band

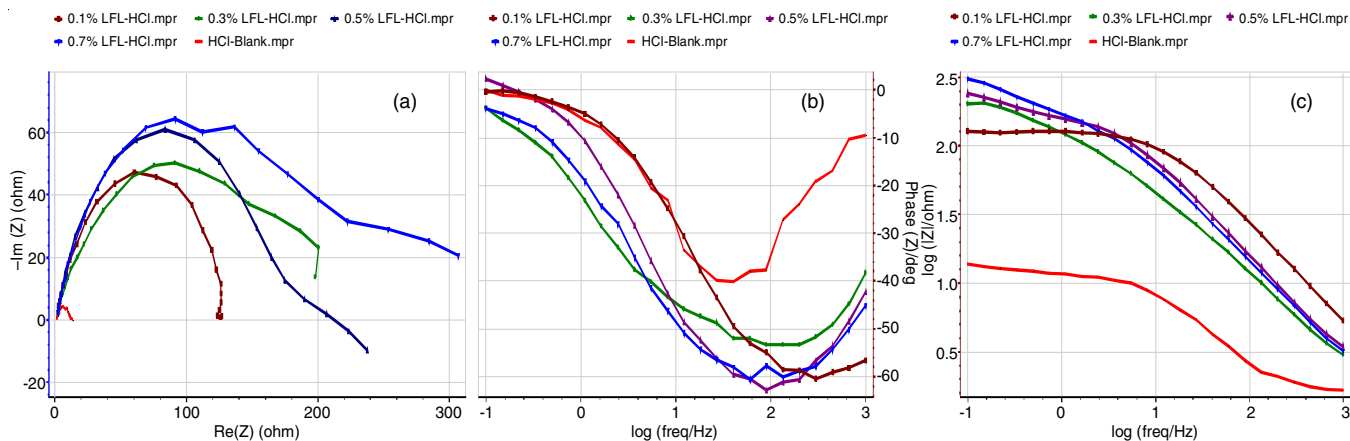


Fig. 7. Nyquist and bode format impedance charts for mild steel in 1 M HCl with and without LFL extract

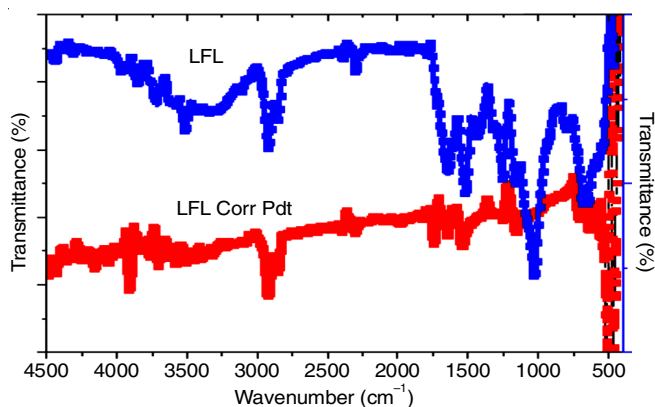


Fig. 8. FTIR spectra of LFL/HCl and corrosion byproducts in 1 M HCl

at 3516 cm^{-1} shifted to 3479 cm^{-1} , whereas the peak at 1643 cm^{-1} shifted to 1705 cm^{-1} . Additionally, the peak at 1524 cm^{-1} is found to be shifted to 1538 cm^{-1} . These major peak shifts clearly demonstrated that the inhibitors interacted with the metal surface.

UV-visible studies: The UV-visible analysis of before and after immersion of mild steel in 1 M HCl is shown in Fig. 9. Main absorption peaks at wavelengths of 410, 450, 680 and 848 nm appeared in UV-visible spectra. Following immersion in mild steel, the plant extract under investigation showed an increase in absorbance. These bands may arise from transitions like $\pi\text{-}\pi^*$ and $n\text{-}\pi^*$, which have a strong charge transfer character. After 3 h of immersion in mild steel, a shift in the position of the absorption maximum or a change in the absorbance values

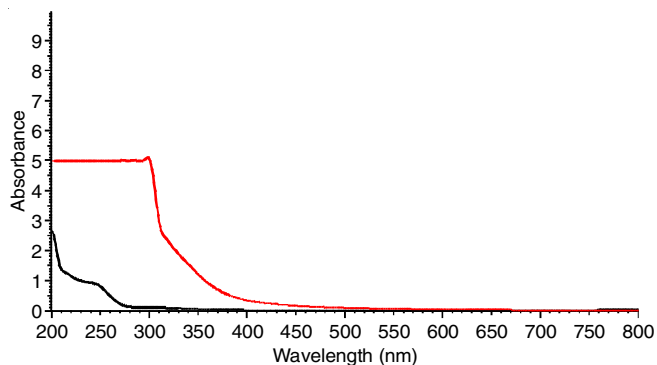


Fig. 9. UV-visible spectra of corrosion products in 1 M HCl and LFL/HCl

indicates the formation of a complex between Fe^{2+} and the phytoconstituents of the plant extract. The carbonyl groups in the combination with Fe are responsible for the band in the 470–490 nm region. It is clear that a blue shift took place close to the $n\text{-}\pi^*$ and $\pi\text{-}\pi^*$ transitions' band maximums, indicating that the carbonyl groups are stable in the presence of iron [29].

SEM studies: SEM images for 3 h of immersion for mild steel, mild steel in 1 M HCl and mild steel in 1 M HCl with 0.7% LFL, respectively. After immersion in the uninhibited solutions, the extensively corroded surface morphology was evident due to the corrosive attack of the acid solution. The corrosive conditions caused metal breakdown, which severely degraded the mild steel surface. However, the presence of LFL significantly reduced the surface roughness of mild steel (Fig. 10), demonstrating the additive's ability to suppress corrosion in 1 M HCl. In addition, there are similar characteristics that are associated with the formation of abrasive scratches [30].

EDX studies: After immersing the carbon steel for 3 h in a 1 M HCl test solution, both with and without a 0.7% inhibitor extract, the elements on the surface were identified using EDX spectra. The EDX spectrum (Fig. 11a) shows the composition of a pure mild steel surface that has not been exposed to acid or inhibitor treatment, which indicate that free carbon steel did not rust. Fig. 11b displays the the EDX analysis of the surface composition of carbon steel following a 3 h immersion in 1 M HCl test solution whereas Fig. 11c depicts the EDX examination of the mild steel surface in the presence of 0.7% LFL and following immersion in a 1 M HCl test solution. Since the molecules of the inhibitor extract contain oxygen atoms, additional lines in the spectra indicate the presence of oxygen. Since there are no oxygen signals on the specimen surface when exposed to without inhibitor in HCl medium, the active chemical components of the extract attached themselves to the metal surface to form a coated layer.

3D Optical profilometer: Upon completion of the 3D optical profilometer image analysis to determine the average roughness (R_a) and root-mean-square roughness (R_q) of the surface, as displayed in Table-7, the following observations were made. Fig. 12a illustrates the surface topography of a pristine metal surface, revealing R_q and R_a values of $3.140\text{ }\mu\text{m}$ and $2.558\text{ }\mu\text{m}$, respectively, for the polished mild steel reference

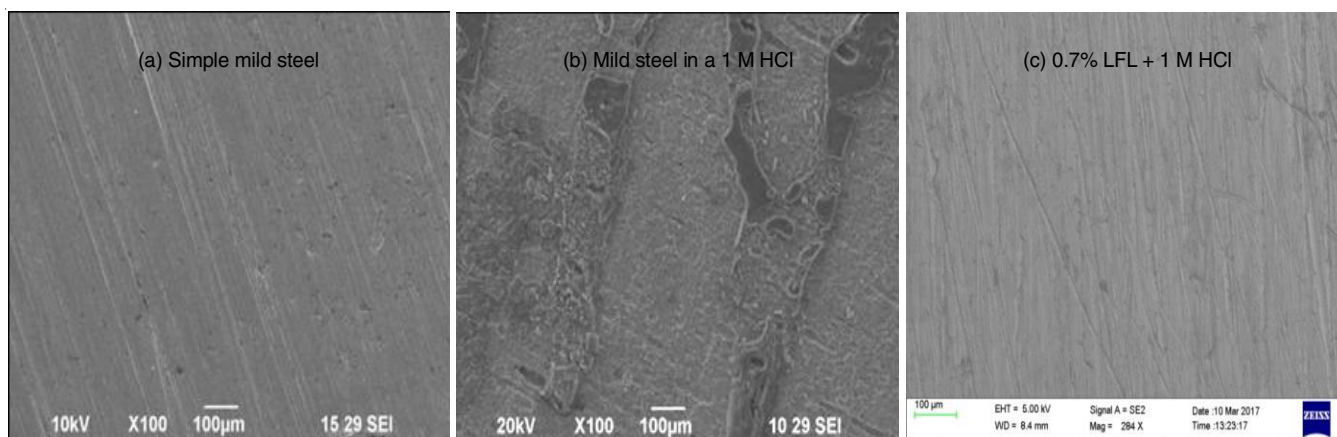


Fig. 10. Mild steel SEM morphologies in HCl with 0.7% LFL present

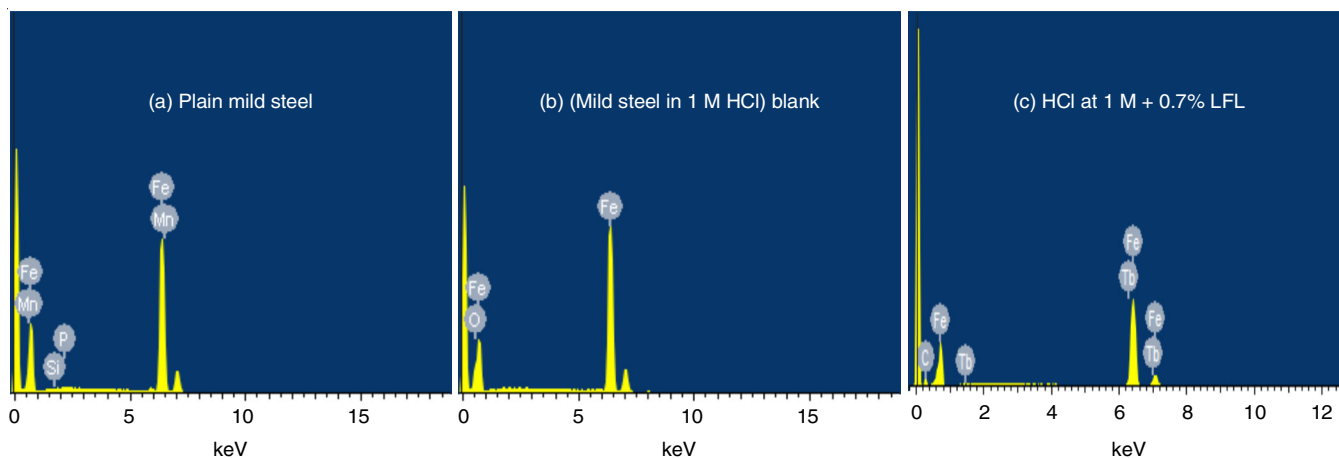


Fig. 11. EDX examination of mild steel in HCl with 0.7% LFL

TABLE-7
AVERAGE ROUGHNESS (Ra) AND ROOT MEAN SQUARE ROUGHNESS (Rq) VALUES FOR MILD STEEL IMMERSED IN 1 M HCl AT VARIOUS LFL EXTRACT CONCENTRATIONS

Samples	Ra (μm)	Rq (μm)
Simple mild steel	2.558	3.140
Mild steel in 1 M HCl	17.2	22.3
Mild steel in 1 M HCl + 0.7% LFL	8.4	11.1

sample. In contrast, Fig. 12b displays the corroded metal surface immersed in 1 M HCl without inhibitor, exhibiting height values of 22.3 μm (Rq) and 17.2 μm (Ra) for the mild steel surface. These findings suggest that the corrosion in the mild steel leads to a rougher surface compared to the polished metal reference. Fig. 12c depicts the mild steel surface in the presence of 0.7% inhibitor following immersion in 1 M HCl, displaying reduced values of 11.1 μm (Rq) and 8.4 μm (Ra). Notably, the presence of the inhibitor significantly decreases Rq and Ra, indicating a smoother surface when the environment is inhibited. This smoother surface is attributed to the formation of a dense layer of Fe²⁺ complex on the metal surface and thus effectively prevent the mild steel corrosion.

Conclusion

The findings of this study demonstrated the impressive potential of *Leucophyllum frutescens* leaves extract as a green corrosion inhibitor to achieve the maximal inhibition of 98.2% in 1 M HCl medium. The extract demonstrated resilience to temperature variations, exhibiting inhibitory efficacy ranging from 65.7% at ambient temperature to 91.2% in 1 M HCl. The inhibitors investigated in this study exhibited heterogeneous monolayer formation on the electrode surface, according to Langmuir and Temkin adsorption isotherms. The calculated thermodynamic parameters indicated a physisorption process, spontaneous adsorption and disruption of solvent entropy, suggesting an appropriate mechanism for inhibition. Changes in the R_p and R_{ct} values, accompanied by reductions in I_{corr} and C_{dl} values, suggest adsorption onto the mild steel surface, followed by a monolayer adsorption process. Maximum efficiency of 83.7% and 98.1% was observed with I_{corr} and R_p in 1 M HCl. Moreover, the environmentally friendly inhibitors evaluated

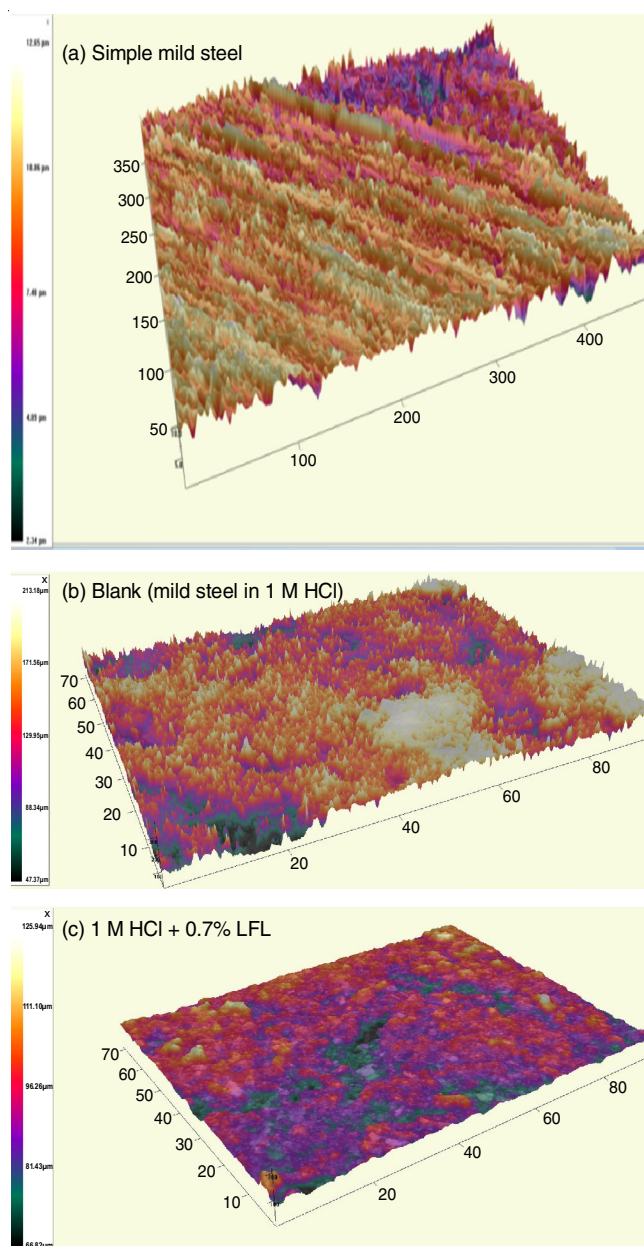


Fig. 12. 3D Optical profilometer images of MS in HCl with 0.7% LFL

in this study exhibited mixed-type inhibitory behaviour, proving to be both economically viable and environmentally benign. Thus, the *L. frutescens* leaves extract emerges as an exceptionally cost effective, environmentally friendly and sustainable inhibitor solution.

ACKNOWLEDGEMENTS

The authors express their gratitude to their respective Institutions for providing the necessary experimental facilities and support.

CONFLICT OF INTEREST

The authors declare that there is no conflict of interests regarding the publication of this article.

REFERENCES

- O. Kaczerewska, R. Leiva-Garcia, R. Akid and B. Brycki, *J. Mol. Liq.*, **247**, 5 (2017); <https://doi.org/10.1016/j.molliq.2017.09.103>
- M. Goyal, S. Kumar, I. Bahadur, C. Verma and E.E. Ebenso, *J. Mol. Liq.*, **256**, 565 (2018); <https://doi.org/10.1016/j.molliq.2018.02.045>
- D.S. Chauhan, M. Quraishi, A. Sorour, S.K. Saha and P. Banerjee, *RSC Adv.*, **9**, 14990 (2019); <https://doi.org/10.1039/C9RA00986H>
- A.S. Fouda, A. El-Askalany, A. El-Habab and S. Ahmed, *J. Bio Tribocorros.*, **5**, 56 (2019); <https://doi.org/10.1007/s40735-019-0248-2>
- R. Yildiz, *Corros. Sci.*, **90**, 544 (2015); <https://doi.org/10.1016/j.corsci.2014.10.047>
- C. Verma, M. Quraishi, L.O. Olasunkanmi and E.E. Ebenso, *RSC Adv.*, **5**, 85417 (2015); <https://doi.org/10.1039/C5RA16982H>
- A. Nahlé, R. Salim, F. El Hajjaji, M.R. Aouad, M. Messali, E. Ech-Chihbi, B. Hammouti and M. Taleb, *RSC Adv.*, **11**, 4147 (2021); <https://doi.org/10.1039/D0RA09679B>
- A. Espinoza-Vázquez, F.J. Rodríguez-Gómez, I.K. Martínez-Cruz, D. Ángeles-Beltrán, G.E. Negrón-Silva, M. Palomar-Pardavé, L.L. Romero, D. Pérez-Martínez and A.M. Navarrete-López, *R. Soc. Open Sci.*, **6**, 181738 (2019); <https://doi.org/10.1098/rsos.181738>
- E.E. Oguzie, V.O. Njoku, C.K. Enenebeaku, C.O. Akalezi and C. Obi, *Corros. Sci.*, **50**, 3480 (2008); <https://doi.org/10.1016/j.corsci.2008.09.017>
- M.F. Lebrini, F. Robert and C. Roos, *Int. J. Electrochem. Sci.*, **5**, 1698 (2010); [https://doi.org/10.1016/S1452-3981\(23\)15422-8](https://doi.org/10.1016/S1452-3981(23)15422-8)
- P.C. Okafor, M.E. Ikpi, E. Uwah, E.E. Ebenso, U.J. Ekpe and S.A. Umoren, *Corros. Sci.*, **50**, 2310 (2008); <https://doi.org/10.1016/j.corsci.2008.05.009>
- H. Wei, B. Heidarshenas, L. Zhou, G. Hussain, Q. Li and K. (Ken) Ostrikov, *Mater. Today Sustain.*, **10**, 100044 (2020); <https://doi.org/10.1016/j.mtsust.2020.100044>
- M.A. Quraishi, A. Singh, V.K. Singh, D.K. Yadav and A.K. Singh, *Mater. Chem. Phys.*, **122**, 114 (2010); <https://doi.org/10.1016/j.matchemphys.2010.02.066>
- P.R. Vijayalakshmi, R. Rajalakshmi and S. Subhashini, *J. Chem.*, **22**, 4537 (2010); <https://doi.org/10.1155/2010/453694>
- E.E. Oguzie, C.K. Enenebeaku, C.O. Akalezi, S.C. Okoro, A.A. Ayuk and E.N. Ejike, *J. Colloid Interface Sci.*, **349**, 283 (2010); <https://doi.org/10.1016/j.jcis.2010.05.027>
- I. Ahmad, S. Ahmed, E. K Akkol, H. Rao, M. N. Shahzad, U. Shaukat, A. Basit and M Fatima, *S. Afr. J. Bot.*, **148**, 200 (2022); <https://doi.org/10.1016/j.sajb.2022.04.038>
- G.M. Molina-Salinas, V.M. Rivas-Galindo, S. Said-Fernández, D. C. Lankin, M.A. Munoz, P. Joseph-Nathan, G.F. Pauli and N. Waksman, *J. Nat. Prod.*, **74**, 1842 (2011); <https://doi.org/10.1021/np2000667>
- G.P. Miller, W.W. Bhat, E.R. Lanier, S.R. Johnson, D.T. Mathieu and B. Hamberger, *Plant J.*, **104**, 693 (2020); <https://doi.org/10.1111/tpj.14957>
- A.A. Thabet, I.M. Ayoub, F.S. Youssef, E. Al Sayed and A.N.B. Singab, *Nat. Prod. Res.*, **36**, 4704 (2022); <https://doi.org/10.1080/14786419.2021.2000981>
- A.J. Harborne, *Phytochemical Methods A Guide to Modern Techniques of Plant Analysis*, Springer Nature (1998).
- O.A. Akinbulumo, O.J. Odejebi and E.L. Odekanle, *Results Mater.*, **5**, 100074 (2020); <https://doi.org/10.1016/j.rinma.2020.100074>
- P.S. Neriyaana and V.D. Alva, *Chem. Afr.*, **3**, 1087 (2020); <https://doi.org/10.1007/s42250-020-00190-z>
- A. Berrissoul, E. Loukili, N. Mechbal, F. Benhiba, A. Guenbour, B. Dikici, A. Zarrouk and A. Dafali, *J. Colloid Interface Sci.*, **580**, 740 (2020); <https://doi.org/10.1016/j.jcis.2020.07.073>
- A.O. Yuce, *Met. Mater. Int.*, **26**, 456 (2020); <https://doi.org/10.1007/s12540-019-00509-7>
- M. Alimohammadi, M. Ghaderi, A. Ramazani S.A and M. Mahdavian, *Sci. Rep.*, **13**, 3737 (2023); <https://doi.org/10.1038/s41598-023-30571-6>
- A.K. Singh, B. Chugh, M. Singh, S. Thakur, B. Pani, L. Guo, S. Kaya and G. Serdaroglu, *J. Mol. Liq.*, **330**, 115605 (2021); <https://doi.org/10.1016/j.molliq.2021.115605>
- B. Chugh, A.K. Singh, A. Chaouiki, R. Salghi, S. Thakur and B. Pani, *J. Mol. Liq.*, **299**, 112160 (2020); <https://doi.org/10.1016/j.molliq.2019.112160>
- I. Ichchou, L. Larabi, H. Rouabhi, Y. Harek and A. Fellah, *J. Mol. Struct.*, **1198**, 126898 (2019); <https://doi.org/10.1016/j.molstruc.2019.126898>
- A.A. Fadhil, A.A. Khadom, S.K. Ahmed, H. Liu, C. Fu and H.B. Mahood, *Surf. Interfaces*, **20**, 100595 (2020); <https://doi.org/10.1016/j.surfin.2020.100595>
- F. Kaya, R. Solmaz and H.I. Geçibesler, *J. Ind. Eng. Chem.*, **122**, 102 (2023); <https://doi.org/10.1016/j.jiec.2023.02.013>